

P1.10 COMPARISON OF IN-SITU ELECTRIC FIELD AND RADAR DERIVED PARAMETERS FOR STRATIFORM CLOUDS IN CENTRAL FLORIDA

Monte Bateman^{1,*}, Douglas Mach², Sharon Lewis³, James Dye³, Eric Defer³, C.A. Grainger⁴, Paul Willis⁵, Francis Merceret⁶, Dennis Boccippio⁷, and Hugh Christian⁷

¹Universities Space Research Association, Huntsville, AL

²University of Alabama in Huntsville

³National Center for Atmospheric Research, Boulder, CO

⁴University of North Dakota, Grand Forks

⁵NOAA/Hurricane Research Division, Coral Gables, FL

⁶NASA/Kennedy Space Center, FL

⁷NASA/Marshall Spaceflight Center, Huntsville, AL

1. ABSTRACT

Airborne measurements of electric fields and particle microphysics were made during a field program at NASA's Kennedy Space Center. The aircraft, a Cessna Citation II jet operated by the University of North Dakota, carried six rotating-vane style electric field mills, several microphysics instruments, and thermodynamic instruments. In addition to the aircraft measurements, we also have data from both the Eastern Test Range WSR-74C (Patrick AFB) and the U.S. National Weather Service WSR-88D radars (primarily Melbourne, FL). One specific goal of this program was to try to develop a radar-based rule for estimating the hazard that an in-cloud electric field would present to a vehicle launched into the cloud. Based on past experience, and our desire to quantify the mixed-phase region of the cloud in question, we have assessed several algorithms for integrating radar reflectivity data in and above the mixed-phase region as a proxy for electric field. A successful radar proxy is one that can accurately predict the presence or absence of significant electric fields. We have compared various proxies with the measured in-cloud electric field strength in an attempt to develop a radar rule for assessing launch hazard. Assessment of the best proxy is presented.

2. INTRODUCTION

Launch vehicles can be severely damaged by lightning strikes. Thus, it is critical for them to avoid areas where they can trigger lightning. To avoid conditions where lightning may be triggered, NASA created a set of rules called the Lightning Launch Commit Criteria (LLCC). The "modern day" LLCCs were written in response to an incident that occurred in

1987 where an Atlas/Centaur-67 rocket, carrying a Navy communication satellite, triggered lightning about 48 s after launch. The lightning current ultimately resulted in a hard-over yaw command that caused an excessive angle of attack, large dynamic loads, and ultimately the destruction of the vehicle. Since the modern LLCCs were put in place in the early 1990s, NASA (and others) have nearly 15 years of experience using these rules. The operational community have noted that several LLCCs seem to be overly conservative and may have reduced launch availability without an increase in launch safety. The rules in question specifically dealt with anvils, layered clouds, and thunderstorm debris clouds. The latest Airborne Field Mill (ABFM) project was given the task of collecting and analyzing data on these specific cloud types with the goal of recommending improved LLCCs.

The ABFM Project was conducted near the Kennedy Space Center (KSC) during June 2000, February 2001, and May/June 2001. It was a cooperative project among NASA/KSC, National Center for Atmospheric Research (NCAR), NASA/Marshall Space Flight Center (MSFC), University of North Dakota (UND), University of Arizona, and the NOAA/National Hurricane Lab. The goal of the project was to investigate the microphysical, radar, and electrical properties of anvils, debris clouds, and layered clouds that violate (or might violate) the current LLCCs and how these properties change with time. Airborne measurements of the 3-D electric fields and associated cloud and precipitation particle content were made using the UND Citation II jet aircraft. These airborne measurements were coordinated with measurements from the WSR-74C radar at Patrick Air Force Base and the National Weather Service NEXRAD WSR-88D radar in Melbourne, Florida. Many of the airborne measurements were made within range of the KSC Light-

* Corresponding author address: Monte Bateman, NASA-MSFC, Mail Code XD11, Huntsville, AL 35805; e-mail: monte.bateman@msfc.nasa.gov

ning Ranging and Detection (LDAR) system, the KSC Cloud-to-Ground Lightning Sensing System (CGLSS), and the KSC surface electric field mill network allowing us to know when and where lightning was occurring and when electric fields were enhanced at the ground near KSC.

This paper focuses on one aspect of the ABFM project: developing a radar product that can act as a sufficient proxy for the electric fields in anvil and debris clouds. Since the electric field in a cloud is carried on charged cloud particles, and radar is able to detect those particles, it should be possible to create a radar parameter that can approximate, or at least indicate, the presence of electric fields. Several candidate products were computed and compared. This paper details the process and the results of the comparison, and presents the best solution to the problem.

3. TERMINOLOGY

We need to define how we “grade” a radar proxy for the electric field. With a single parameter rule, there are four possibilities. If a radar product in question (proxy) indicates a hazardous electric field and the field mills measure a field that is not hazardous, we call this a *false alarm*. If the radar proxy indicates a non-hazardous electric field and the field mills measure a hazardous field, we call this a *failure to detect*. If the radar proxy predicts no hazard and the field mills confirm no hazardous fields or the proxy predicts a hazard and the field mills confirm the hazardous fields, we call these conditions a *success*. The goal of any proxy rule is to have as few cases as possible in the first two categories (i.e., as few false alarm and failure to detect cases as possible) while having as many as possible in the last two categories (i.e., all hazardous or safe fields indicated by the radar proxy).

Because the consequences of a failure to detect case is so great for LLCCs (i.e., loss of launch vehicle), any rule that may be implemented must have no failures to detect. Because of this, in the statistical models presented later, we must set the Probability of Detection (POD) to 1. This usually causes an increase in the false alarm rates (FAR) of a given rule.

4. INSTRUMENTATION

During the ABFM program, the UND Citation carried electric field mills, an array of microphysics instruments, thermodynamic and wind sensors. The navigation recorder provided aircraft attitude, position and heading. For safety reasons, the Cita-

tion was limited to penetrating reflectivity of up to 35dBZ, and the aircraft has a service ceiling of 13 km.

This complement of instruments gave us the ability to measure variables relevant to storm electrification. We were also able to geolocate the aircraft into the radar data and (in post-flight processing) place our *in-situ* measurements into the larger storm context. Also during post-processing, we used the radar data and aircraft observer information to classify our case studies by cloud type.

4.1 Data Collected

Microphysics. The Citation carried several microphysical imaging instruments, including: PMS probes FSSP, 1-DC, 2-DC, and SPEC instruments HVPS and CPI. It also carried a PMS King probe that measured liquid water content and a Rosemount icing rate meter that measured super-cooled liquid water content. These data were continuously recorded during flight.

Electric Field. The Citation carried 6 electric field mills. Each mill output was continuously recorded during flight. Post-flight, linear combinations of the 6 mill outputs were generated to create vector field components \mathbf{E} (E_x, E_y, E_z), using the calibration technique of Mach and Koshak (2003).

Shown in Fig. 1 are the time-series plots for the x , y , and z components of \mathbf{E} . The fourth trace, E_q , shows the field due to charge on the aircraft. Shown in Fig. 2 are pairwise coordinate plots of \mathbf{E} : xy , yz , and xz along with aircraft track.

Radar. During the ABFM program, there were two primary radars that routinely archived data for the program’s use. These included the WSR-74C radar at Patrick Air Force Base (Cocoa Beach, FL) and the NWS WSR-88D at Melbourne, FL. These radars are of the most interest, as they are used for launch support.

5. FLIGHT TRACK STRATEGIES

The clouds that were the subject of the recent ABFM program fall into several major categories. In each case, the clouds were not considered part of an active convective system. Actively convective systems are the subject of a distinct set of LLCC rules and were not part of this investigation. Our investigation focused on the non-convective clouds such as anvils, detached anvils, debris clouds, or layered clouds.

5.1 Long anvils attached to active convection

Summertime thunderstorms in Florida can create anvils that are 100–200 km long. Because these anvils are still attached to the parent thunderstorm, they are LLCC violations. One unanswered question is: *How far away from the parent storm must a vehicle be before it can safely penetrate the anvil without triggering lightning?* Since the electric field in a cloud decays with time (Willett and Dye, 2003; Dye et al., 2003), and we are fairly certain active charge separation does not occur in these anvils, then a “ruler and stopwatch” approach can be used in assessing the safety of such clouds. Existing LLCCs use this approach; our goal is to replace such rules with radar-based rules. Thus, we need a radar product that can be used as a proxy for **E** in anvils attached to active convection.

In order to address this question, we flew tracks along the main (upwind/downwind) axis of several attached anvils, from the tip towards the parent storm and back. Electric field was measured, and the point at which it crossed the hazardous threshold (~ 10 kV/m) was noted. By measuring distance from the convective tower and the anvil-level winds, we can determine the time (age of cloud volume) necessary for the electric field to have decayed to non-hazardous levels. This was compared to various candidate radar products. We also flew transverse tracks across the anvil to see if the field decay was related to distance from cloud edge, perhaps due to mixing in of non-cloudy air.

5.2 Long-lived, detached anvils

With typical summertime dewpoints at anvil altitudes, Florida thunderstorms can create anvils that exist for many hours after the parent storm has dissipated. The current LLCC rules require that detached anvils cannot be penetrated for three hours after detachment from the parent storm. So, the question is: *How long do we have to wait until it is safe to launch a space vehicle through a detached anvil?* As in the case for attached anvils, an alternate approach is to attempt to use the radar data to determine when the anvil is safe to penetrate.

In order to address this question, we flew similar tracks as described in section 5.1. Flying along the main axis lets us measure electric field vs. age of cloud; flying across the anvil lets us measure electric field vs. decay from mixing.

5.3 Thunderstorm Debris Clouds

When typical Florida thunderstorms dissipate, they often leave cloud remnants that can affect launch

availability for hours. As in the anvil case, the LLCC requires that debris clouds not be penetrated for 3 hours after they separate from their parent storm (or when the parent storm dissipates). So, the question for these cloud remnants is similar to those above: *Can we find a radar product to replace the stop-watch approach?*

In order to answer this question, we flew similar tracks as described in section 5.1. Flying along the main axis lets us measure electric field vs. age of cloud; flying across the debris cloud lets us measure electric field vs. decay from mixing.

5.4 Layered Clouds

Often in wintertime conditions, cloud layers will develop in the KSC area. These cloud layers may or may not be connected (currently or at one time) to convective thunderstorms. The current LLCC rules use thickness and altitude parameters to determine if a layered cloud can or can not be penetrated. Since these clouds are very long lived and do not decay much with time, the study approach for these clouds is to find a radar based parameter that can be a proxy for the electric field in the layered clouds.

To help determine any such parameter, we flew the aircraft in the layered clouds to determine the fields as a function of radar data. We also flew “vertical profiles” of the clouds to determine if ground based measurements could be used as a proxy for the fields in the clouds.

6. DATA ANALYSIS

6.1 Data Reduction

We were provided with NEXRAD ARC-II data (KMLB, primarily) from the NWS and NCDC; the WSR-74C data were recorded on site at KSC. Data from both radars were gridded with NCAR’s SPRINT program using a $(1 \times 1 \times 1)$ km grid spacing. To verify the relative calibration of the two radars, we compared the reflectivity values from both radars on a few storms that were equidistant from both radars. The comparison showed that the reflectivity values matched within about 3 dBZ.

Aircraft data were geolocated using the GPS system on the aircraft. All data recorded on the Citation were reduced to a time-series matrix. Any measurement or product could then be plotted onto the gridded radar data for comparison. We developed many visualization tools to help analyze this unique dataset.

6.2 Comparing E with radar: Our strategy

Starting from a basic understanding of charge microphysics, we sought to create algorithms for generating radar products that might correlate with electric field. We start with the assumption that charge is most efficiently separated when ice crystals interact with graupel pellets in a deep mixed-phase region. This led us to try many possible algorithms.

Since the mixed-phase region seems to be the critical region for charge separation in clouds, we set 0°C as the lower limit for our radar domain. There was very little incentive to include clouds that were composed of only liquid water. Very few (if any) clouds in the KSC region become electrified when they are totally composed of liquid water. Although the cloud mass above the mixing layer does not contribute to the separation of charge as much as the mixed layer, it does contain cloud components that were lifted up from the mixed phase layer. Therefore, our radar volumes included components from the freezing level to cloud top. For summertime in Florida, 0°C typically is found at about 5 km altitude.

We wanted to only include radar volume that was relevant to the electric field measurement. Since E falls off as r^{-2} , we want to only include cloud volumes that may be influencing the electric field. Within the gridded radar data, we considered subsets that were centered on the gridbox that contained the aircraft. We used various influence ranges that extended a few boxes from center (the aircraft's box) in each compass direction.

So the question is: What is the appropriate size for the influence box? As we move away from the aircraft, the charge that exists on the cloud in successively further boxes diminishes rapidly in its contribution to the field we measure at the aircraft. For example, the third box out from the aircraft contributes less than 5% to the measured electric field. However, due to geolocation errors between the radars and the aircraft, we could have a difference of 1–2 km in location, so to ensure we are including the cloud that is at or near the aircraft, we need to include another 1–2 boxes to our influence range parameter. This led us to use a radar influence domain that extended 5 km in each direction from the aircraft, or what we called the (11×11) box.

One of the challenges in computing radar products is accommodating scan gaps. Scan gaps occur when subsequent radar beams (elevation or tilt angle) do not touch or overlap with previous beams. In the interest of speed, some elevation angles have

been skipped. This allows the scan volume to complete in a shorter amount of time, but it leaves cones of unsampled space, or missing data. The problem is that we have no way of differentiating between (a) unsampled space and (b) sampled space that had no return. Because of beam geometry, scan gaps are worst close to the radar antenna. So, any algorithm we create must prove to be robust relative to scan gaps.

6.3 Radar Algorithms

Our desire was to create radar products that might be a good proxy for E . We know that charge is stored on cloud particles. Since it is unlikely active charge separation is occurring in the anvil and debris clouds we are studying (no updraft, insignificant LWC), we are basically looking at a charge storage issue (capacitor). So, the more cloudy material that exists colder than 0°C , the more charge a particular anvil is likely to be able to hold.

The radar measures reflectivity and cloud depth. Both contribute to the amount of cloud particles in a volume. So the requirements for the parameter are that it measures both cloud density and depth and is robust to scan gaps. Since no single parameter could meet all requirements, the task was in picking ones that met as many as possible. All algorithms were calculated over the (11×11) box, or 121 columns.

1. Volume Average Reflectivity. The simplest product to calculate is simply the bulk average of the entire domain volume. This has the advantage of filling-in the radar scan gaps, but because an entire volume is reduced to a single average value, it has the disadvantage of destroying depth-of-cloud information.

2. Volume Average Reflectivity \times thickness. Same as above, but here we multiplied by an average cloud thickness to put the depth-of-cloud information "back in." This has a problem with over-smoothing, as we are multiplying one average by another.

3. Column-wise Integrated Reflectivity. Another approach is to simply add up (integrate) all the reflectivity values in each column, and then sum all the column values. This algorithm is superior to averaging, because it preserves depth-of-cloud information. However, the problem with this approach is that scan gaps can significantly alter the results.

4. Column Average \times Cloud Thickness. Integrated reflectivity doesn't handle scan gaps well,

but column-wise averaging does. However, column-wise averaging loses the depth information. As it turns out, if we multiply the column-wise average times the cloud thickness for that column (thus putting the depth-of-cloud information “back in”), we get a quantity that is very similar to the integrated reflectivity that is also robust to scan gaps. It also is easier to implement in real-time radar software.

6.4 Comparison Methodology & Models

In order to compare many (~ 30) different candidate radar algorithms versus measured **E**, we used a graph called the receiver operating characteristic, or ROC curves. These curves plot the probability of detection (POD) vs. the false alarm rate (FAR) for specific models (radar product algorithms). It is a parametric plot of False Alarm Rate (or Ratio) vs Probability of Detection, as a decision threshold is varied across its dynamic range. It is derived by computing standard contingency tables for every value of the decision threshold. The decision threshold is applied to the continuous variable used to assign a “detection.” This can be an observed parameter (the “model” is $x > \text{threshold}$), model output (the “model” is $f(x) > \text{threshold}$), etc. In classification neural networks whose output is a 0–1 probability, the decision threshold is the probability above which we claim the model predicts a “detection” (this need not be 0.5).

“Better” models have ROC curves which bunch more towards the upper left corner of the plots (high POD, low FAR). The area under a ROC curve provides a scalar measure of overall model performance, and loosely, “versatility” (since different end-users may wish different POD/FAR tradeoffs). By reporting skill parametrically via a ROC curve, we avoid pre-determining the decision threshold and hence POD/FAR. This differs from conventional scalar statistics such as the Critical Success Index (CSI) or Heidke Skill Score (HSS); these correspond to a *single* decision threshold; i.e., each point on a ROC curve has its own CSI/HSS. (To merge the two, the point on the ROC curve which has the highest CSI/HSS can optionally be highlighted, or the ROC color-shaded by CSI/HSS, etc).

7. DISCUSSION

Others have shown that a relationship exists in Florida thunderstorms between the volume of cloud in the mixed-phase region and cloud electrification (French et al., 1996). So, we wanted to craft an algorithm that reflected these observations and incorporate what we know about charge microphysics.

One of the products that did a good job of predicting hazardous **E**, was what we call the vertically integrated reflectivity above 0°C, or VIR0C. For each column of gridded radar data, we add up the reflectivity values from 0°C (5km) to cloud top. These values were then contoured, with the aircraft track overplotted in a color code that indicated predicted **E** and measured **E**. In all the anvil cases, the VIR0C parameter worked extremely well (FAR < 30% with POD = 1) in predicting a hazard where one existed. Note that the current anvil rule has a much higher FAR that approaches 80%.

It is understandable why VIR0C would be a good indicator for storms with active convection, but what about anvils? Since VIR0C incorporates depth-of-cloud information and intensity of reflectivity, anvils that are thick and have high reflectivity will also have high VIR0C values. When anvils are formed, the parent storm advects charge into them and is stored. So the question is, how good is that capacitor? It turns out that the qualities that make an anvil a good “storage device” also give it high VIR0C values — thickness and greater reflectivity.

8. CONCLUDING REMARKS

It is important for NASA/KSC to be able to assess the hazard that may exist in a cloud with their existing infrastructure. We have analyzed many algorithms for a radar proxy of **E**. For anvils attached to active convection, anvils detached from their parent cloud, and debris clouds, the so-called VIR0C parameter is a good indicator of potential hazard. However, mainly due to gaps in the existing radar scan strategies, we have looked at other equivalent radar products. By computing a column average reflectivity and multiplying by the thickness of cloud in the column we can produce a good surrogate for VIR0C that is robust to scan gaps and is easier to implement in software.

REFERENCES

- Dye, J., W. Hall, J. Willett, S. Lewis, E. Defer, P. Willis, D. Mach, M. Bateman, H. Christian, C. Grainger, J. Schild, and F. Merceret, 2003: The decay of electric field in anvils: Observations and comparison with model calculations. In *Proc. ICAE, Versaille, France*, 29–32.
- French, J. R., J. H. Helsdon, A. G. Detwiler, and P. L. Smith, 1996: Microphysical and electrical evolution of a florida thunderstorm 1. observations. *J. Geophys. Res.*, **101**(D14), 14327–14334.

Mach, D. and W. Koshak, 2003: General matrix inversion technique for the calibration of electric field sensor arrays on aircraft platforms. In *Proc. ICAE, Paris*.

Willett, J. and J. Dye, 2003: A simple model to estimate electrical decay. In *Proc. ICAE, Versailles, France*, 267–271.

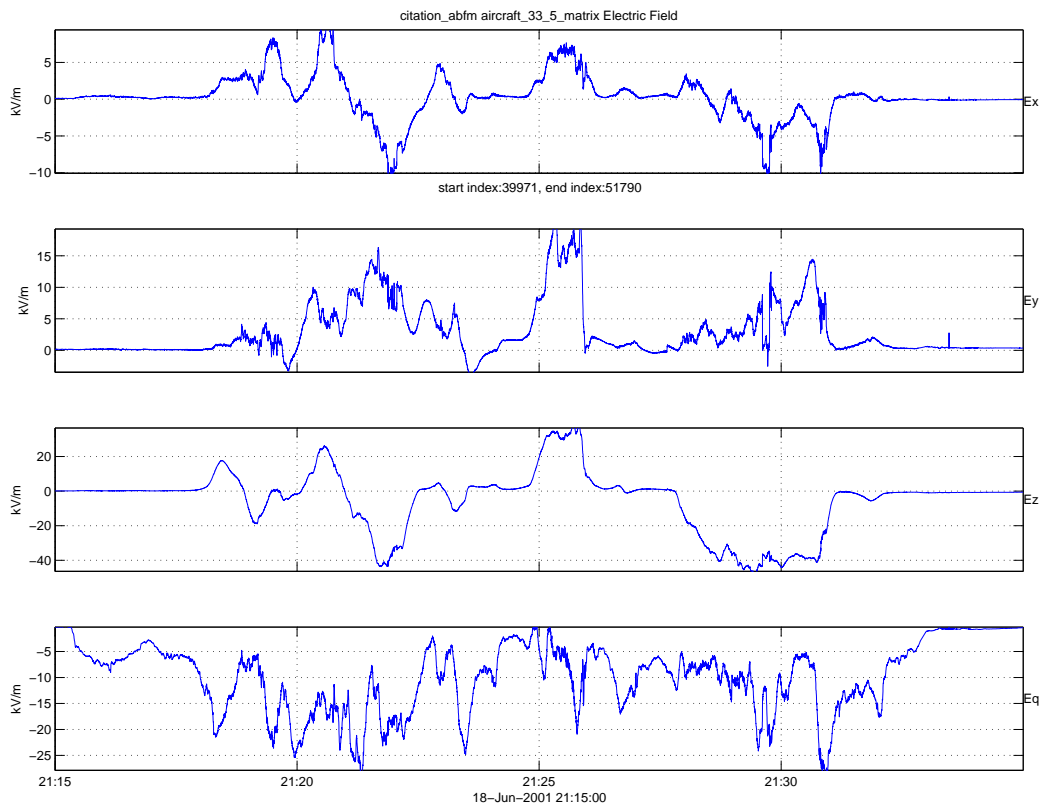


FIG. 1: Time series plot of the electric field during two penetrations of a decaying anvil. The data are from a flight on June 18, 2001. Shown are the x , y , and z components of \mathbf{E} in an aircraft relative sense. Also is what we call E_q , the electric field due to charge on the aircraft.

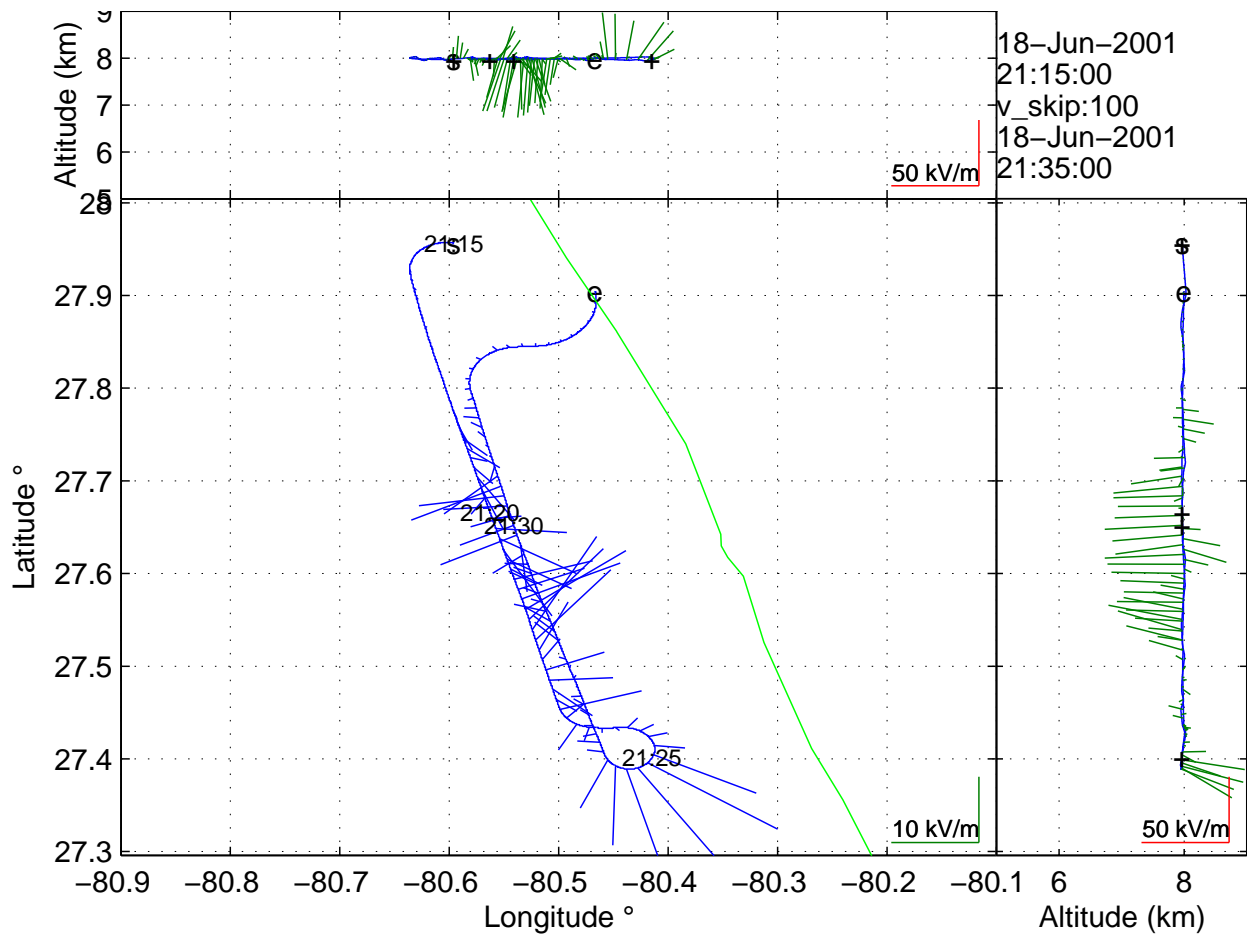


FIG. 2: Plot of aircraft track in xy , yz , and xz and vector electric field in the same plane. Note the scale of the electric field vector are different and are in the lower right-hand corners of each of the three subplots. The start (s) and end (e) of the aircraft track is marked along with minute tick marks.